AUTOMATIC UNHULLED RICE GRAIN CRACK DETECTION BY X-RAY IMAGING

P. A. Kumar, S. Bal

ABSTRACT. *Crack detection of incoming paddy (unhulled rice grain) is an important step in the rice milling industry, as paddy grains with cracks severely affect the milling yield. The present method of crack detection by manually dehusking and examining kernels under light is laborious, time consuming, and highly subjective. The potential of x-ray imaging for paddy grain crack detection was investigated. Algorithms were developed for automatic detection of paddy cracks from the x-ray image. Hough transform was used to determine the cracks in the final segmented image. A graphical user interface (GUI) was developed for displaying the number of cracks in the given x-ray image.*

Keywords. *Cracks, Detection, Paddy, Segmentation, X-ray.*

Quality is an important factor in determining the price of paddy (unhulled rice grain) at the time of procurement in the rice milling industry. Quality of paddy depends on moisture content, foreign material (presence of unwanted material such as stones, straw, etc.), varietal purity, immature grains, discolored or damaged grains, and cracked grains. Cracked grains are caused by rapid or uncontrolled moisture change, particularly absorption of moisture, by mechanical harvest damage or some other postharvest damage, or by sun drying prior to harvest. The presence of cracked grains increases the number of broken grains and reduces the milling yield. Broken grain value is less than half the price of whole grain, so a small number of cracked grains significantly lowers the quality grade of the paddy. In the industry, samples with less than 2% cracked grains are allowed, and samples with greater than 2% are rejected.

The ultimate cause of rice breakage lies within the grain. The proportion of defective grains that break is a function of grain size and shape, along with size, shape, and orientation of cracks, milling system, and degree of milling. At present, paddy samples are dehusked by hand and are examined individually on an illuminated glass plate for the detection of cracks. This method is laborious, inconsistent, time consuming, and highly subjective.

Submitted for review in April 2006 as manuscript number BE 6456; approved for publication by the Biological Engineering Division of ASABE in July 2007.

The authors are **P. Anand Kumar,** Graduate Student, and **Satish Bal, ASABE Member Engineer,** Professor, Department of Agricultural and Food Engineering, Indian Institute of Technology – Kharagpur, West Bengal, India. **Corresponding author:** Satish Bal, Department of Agricultural and Food Engineering, Indian Institute of Technology – Kharagpur, West Bengal, India 721302; phone: 03222-283100; e-mail: satish.bal@gmail.com.

Gunasekaran and Paulsen (1986) and Gunasekaran et al. (1987) developed an image processing algorithm for detecting stress cracks in corn (fine fissures in kernel endosperm underneath the pericarp), which are visible by applying white light in a back-lighting mode. Gunasekaran et al. (1988) used the same technique for detection of soybean seed coat and cotyledon. Wan et al. (2002) developed an automatic grain quality inspection system for rice quality classification, and the classification accuracy for dehusked cracked grains was reported as 87%. He used maximum gray-level difference for classification of cracked rice grains from sound, chalky, dead, immature, and other kernels. In this method of crack detection, dehusking of the paddy was necessary. During dehusking, there is a chance of further cracking of the grain, and the crack detection after dehusking includes these cracks. A crack detection method that eliminates the dehusking process would have great importance in the price determination of paddy during procurement. So far, there is no available published literature on crack detection of unhulled rice kernel by applying image processing techniques.

In recent years, x-ray imaging techniques have proven useful for many agricultural product inspection applications. Thomas et al. (1995) developed a non-destructive x-ray inspection method to detect weevil-infested mango fruits. X-ray images of pistachio nuts containing only nut meat were obtained by digitizing the x-ray films using a film scanner (Casasent et al., 2001). A computer vision system capable of detecting pin holes due to insect damage in almonds was studied by Kim and Schatzki (2001). Tao et al. (2001) detected foreign objects present in deboned poultry. In addition to these studies, soft x-rays have been used extensively for detection of internal defects caused by insect infestation in wheat kernels (Karunakaran et al., 2003a, 2003b, 2004; Haff and Slaughter, 2002, 2004).

The present investigation was carried out to develop a method for paddy grain crack detection using x-ray imaging with the following objectives:

- To investigate the potential of soft x-ray imaging for crack detection of paddy.
- To develop an algorithm for determining the number of vertical and horizontal cracks in a cracked paddy grain.

  ISSN 0001–2351

Materials and Methods

Sample Preparation

Basmati variety paddy grains were used in this investigation. Artificial cracks were developed by soaking and sun drying the paddy samples. The samples (initial moisture content 14% d.b.) were soaked in water at room temperature (24˚C) for 1 h to attain a moisture content of 23%. These samples were then sun dried at an average temperature of 28˚C for two days. The final moisture content of the paddy was 14% (d.b.). With this method, the samples underwent rapid change of moisture and developed cracks (Dong and Mao, 2003).

X-Ray Imaging System

Paddy kernels (four kernels on a single film) were attached to dental x-ray plate (Kodak Industrex E-speed DF film, size 2, Kodak, Inc., Rochester, N.Y.) using adhesive tape and then were x-rayed using a Radon x-ray generator (Radon-House Pvt. Ltd., Calcutta, India) with 0.3 mm thick beryllium window. The Radon x-ray generator had variable energy settings. Clear x-ray images of paddy kernels were obtained at 12 keV, 8 mA, and 10 s exposure time. The exposed x-ray plates were developed in a darkroom. A film scanner (Canoscan 9950, Canon India Pvt. Ltd.) was used to convert the developed plates into digital images. The x-ray images were digitized as monochrome 8-bit images with a spatial resolution of 200 dpi. The soft x-ray images thus obtained were cut into single-kernel images image by the cutting tool available in Adobe Photoshop. The single-kernel soft image was used for image analysis for automatic crack detection and determining the number of cracks.

Image Processing Steps

Figure 1 shows a block diagram of the algorithm for detecting cracks and for determining the number of cracks in a paddy kernel. First, the original x-ray image is preprocessed for noise present in the image. Morphological image enhancement using top-hat transform enhances the high-intensity pixels in the region of cracks, and subtracting this enhanced image from the preprocessed image produces an image with only cracks. However, other high-intensity pixels also get enhanced in this process, which produces some dots in the resulting image after thresholding. A harmonic mean filter, with a threshold value of 127, is then used to produce a final clear binary image of the rice cracks. To find the number of cracks in the image, the pixel coordinates of cracks are transformed from the *x-y* plane to the ρ-θ plane by Hough transform. These steps are described in the following sections.

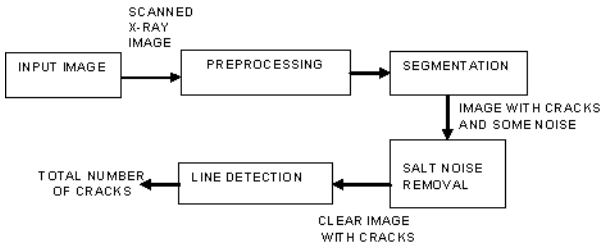

Figure 1. Block diagram of image processing steps.

Preprocessing

Figure 2a shows an original scanned digital x-ray image of a single paddy kernel. The internal cracks are clearly visible for detection and for determination of the number of cracks. To detect the cracks in the image, the image has to be segmented so that only the cracks are visible. To assist segmentation, it is desirable to preprocess the poor quality (e.g., the white spots inside the rice in fig. 2a) x-ray image. For this purpose, the original x-ray image is first converted to a negative image (fig. 2b). The color bar shows the gray values from 0 to 255, and the data cursor shows the gray value of the background as 205. The negative image is then used for image averaging with a square mask of size 10 to reduce the noise. Figure 2c shows the averaged image with fewer white spots.

Segmentation of the X-Ray Image

Similar to the cracks, the air gap between the husk and the kernel has a higher intensity value, while the kernel and the husk have lower intensity values. These factors complicate the segmentation process to extract the cracks by a simple thresholding method. Casasent et al. (2001) used morphological erosion with a structuring disk element to separate the nut meat region from the whole nut, which includes an air gap between the shell and the nut meat. In the case of paddy, the air gap is not uniform, so eroding with a large mask removes some portion of the cracks along the sides, and eroding with a small mask results in some portion of the husk remaining. To overcome this problem, first the contrast of the preprocessed image was enhanced. Top-hat morphological image transform with a structuring square element of size 12 was

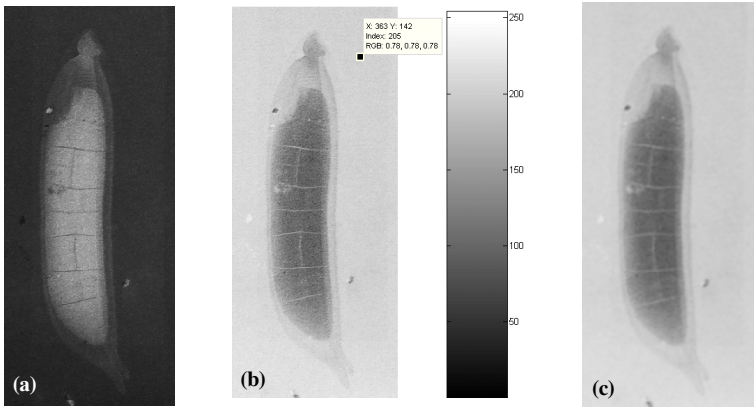

Figure 2. (a) Original scanned x-ray image showing the internal cracks, (b) negative image along with the color bar, and (c) averaged image.

used to enhance the cracked region. Subtracting this enhanced image from the preprocessed image and thresholding produced an image with only cracks.

Top-Hat Transform

The top-hat image transform was performed using equation 1:

$$h = f - (f \circ b) \quad (1)$$

where h is the top-hat transformed image, f is the input image, b is the structuring element, and o indicates the opening of the image. For more details on top-hat transform and opening, refer to the gray-scale morphological processing section in Gonzalez and Woods (2002). As a result of enhancement, pixels having higher-intensity values throughout the image also became enhanced, along with the cracks. Therefore, the resulting image has white spots, which are known as salt noise. This salt noise was removed using harmonic mean filtering.

Harmonic Mean Filtering

Harmonic mean filtering was carried out with a sub-image of 5 × 5 size using equation 2 (Gonzalez and Woods, 2002) to eliminate the white spots that were created by enhancing the image:

$$g(x,y) = \frac{mn}{\sum_{(s,t)\in S_{XY}} \frac{1}{f(s,t)}} \quad (2)$$

where S_{xy} represent the set of coordinates in a sub-image of size $m \times n$ centered at point (x, y), $g(x, y)$ is the filtered image, and $f(x, y)$ is the noisy image.

The resulting binary image produced after harmonic mean filtering with a threshold value of 127 produces a clear image with cracks. The few dots that remain do not effect the determination of the number of cracks. In the final binary image, pixels showing cracks have a value of 1, and background pixels have a value of 0.

Line Detection by Hough Transform

Hough transform was used to find and link line segments from the binary image with cracks. Considering a single point (x_1, y_1), an infinite number of lines pass through that point. All lines passing through this point can be represented by a single sinusoidal curve in the ρ-θ plane (also called the parameter space) for some values of ρ and θ. The equation of the sinusoidal curve is given below:

$$x_1\cos\theta + y_1\sin\theta = \rho \quad (3)$$

Furthermore, a second point in the xy plane (x_2, y_2) also has a line in the parameter space associated with it, and this line intersects the line (eq. 3) at ρ_1 and θ_1, where ρ_1 and θ_1 correspond to the line containing the (x_1, y_1) and (x_2, y_2) points in the xy plane (fig. 3). Hence, representing all points as sinusoidal curves in the ρ-θ plane and then finding the points where a large number of parameter space lines intersect gives the lines in the image.

All pixels with a value of 1 (i.e., pixels representing cracks) are transferred into sinusoidal curves in the ρ θ plane. The points having a maximum number of line intersections (Hough peaks) are calculated using Hough transform (Gonzalez et al., 2004). The ρ and θ values of these Hough peaks give the crack lines in the xy plane.

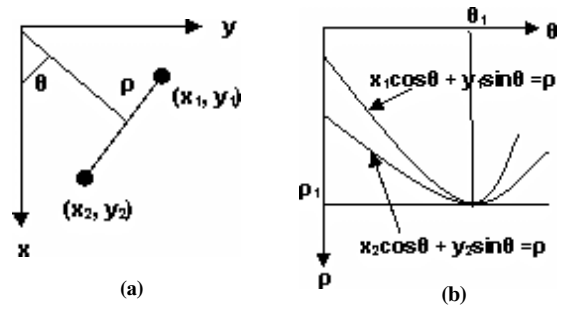

Figure 3. (a) Representation of lines in ρ and θ values in the x-y plane, and (b) sinusoidal curves of points (x_1, y_1) and (x_2, y_2) in the ρ-θ plane. The point of intersection at (ρ_1, θ_1) corresponds to the line joining (x_1, y_1) and (x_2, y_2).

Figure 4. Single crack having three lines, represented by Hough peaks.

The width of the cracks varies from 2 to 6 pixels depending on the size of the crack, and the crack is not always a straight line. Therefore, a single crack in the image may yield more than one peak in the ρ θ plane and may have two or more lines in the xy plane, as shown in figure 4. To find the exact number of cracks, the lines that represent a single crack must be grouped. A programming code was written in Matlab 7 to group peaks that represent the same crack. The midpoint distances of the lines are calculated. If the distance is less than 40 pixels, then these lines are grouped into a single crack. Otherwise, they are treated as different cracks. In addition, lines with θ value greater than 45° are categorized as vertical lines, and lines with a θ value ≤45° are categorized as horizontal lines.

VALIDATION

One hundred grain kernels were used for the validation of the algorithm. After x-raying, the unhulled rice kernels were manually inspected for cracks and compared with the software results for the validation.

RESULTS AND DISCUSSION

Figure 5 shows histogram images of original, negative, averaged, and top-hat enhanced images. It can be clearly seen from figure 5c that averaging improved the image quality. The high peaks at intensity value 205 in figures 5b and 5c indicate the background. The intensity values of the air gap and the cracks vary from 170 to 200. Hence, the single peak at intensity value 188 in the averaged image (fig. 5c) cannot explain the air gap and crack regions separately. The higher-intensity pixels, based on the surrounding sub-image, were enhanced using top-hat transform (fig. 5d). The lower-intensity pixels remain the same in figures 5c and 5d. The resulting image, after subtracting the enhanced image from the averaged image and thresholding, is shown in figure 6a. Salt noise was removed by harmonic mean filtering (fig. 6b).

All the crack points (i.e., those points having 1-valued pixel coordinates from the image with only cracks) were transformed into the ρ-θ plane and represented as sinusoidal

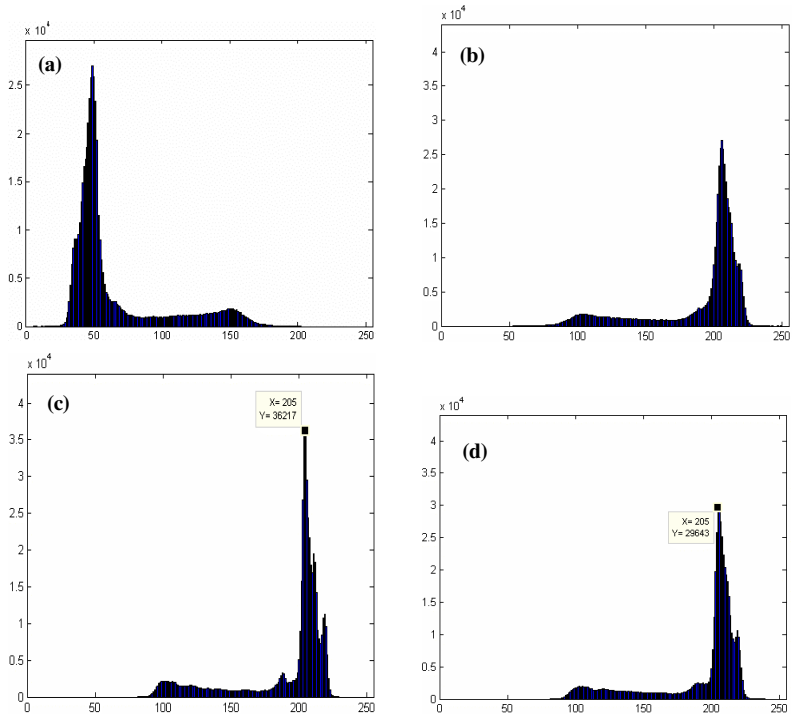

Figure 5. Histograms of the (a) original, (b) negative, (c) averaged, and (d) top-hat enhanced x-ray images.

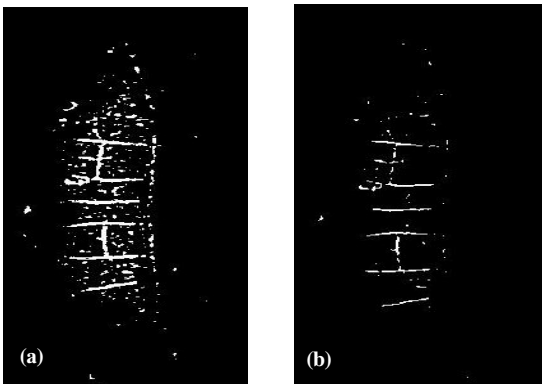

Figure 6. (a) Image with salt noise, and (b) final image showing only cracks.

curves (fig. 7a). Each curve in figure 7a represents a single point of a crack in the image. The small squares in the figure show the maximum intersections (Hough peaks) of the curves. These intersection points with their corresponding ρ and θ values represent the crack lines. Figure 7b show the software results that group the Hough peaks into crack lines and displays the number of vertical, horizontal, and total cracks in the x-ray image. When the algorithm results were compared with the results of manual inspection, the detection of vertical and horizontal cracks was very satisfactory. Of the grains inspected, 98% of the horizontal cracks, 97% of vertical cracks, and 97% of the total cracks were correctly identified.

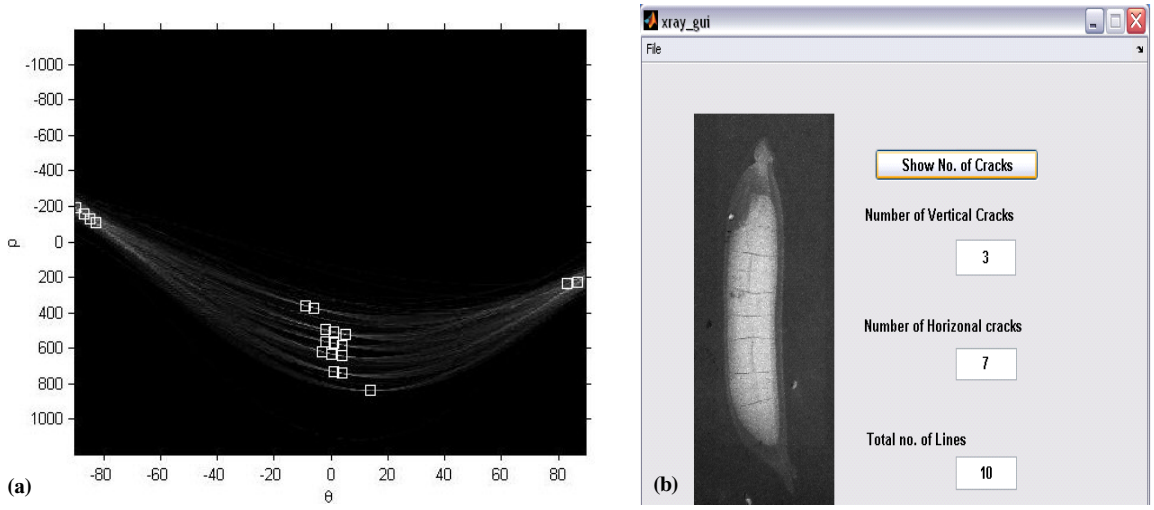

Figure 7. (a) Hough peaks in the ρ-θ plane, and (b) graphical user interface (GUI) displaying the number of horizontal, vertical, and total number of cracks.

Conclusions

X-ray imaging has the potential to find cracks inside paddy. Paddy grain x-ray images produced with 12 keV energy, 8 mA current, and 10 s exposure time by an x-ray generator clearly showed internal details of the paddy, including cracks and the air gap between the husk and the rice kernel. Algorithms were developed for automatic detection of cracks from the x-ray images. A graphical user interface was developed to display the number of vertical, horizontal, and total cracks in the x-ray image with an accuracy of 98%, 97%, and 97%, respectively.

References

Casasent, D., A. Talukder, P. Keagy, and T. Schatzki. 2001. Detection and segmentation of items in x-ray imagery. *Trans. ASAE* 44(2): 337-345.

Dong, L., and Z. Mao. 2003. Experimental study on the microscopic structure of stress cracks of rice kernels after sun drying. ASAE Paper No. 036045. St. Joseph, Mich.: ASAE.

Gonzalez, R. C., and R. E. Woods. 2002. *Digital Image Processing.* 2nd ed. Singapore: Pearson Education.

Gonzalez, R. C., R. E. Woods, and S. L. Eddins. 2004. *Digital Image Processing using MATLAB.* Singapore: Pearson Education.

Gunasekaran, S., and M. R. Paulsen. 1986. Automatic, nondestructive detection of corn kernel defects. In *International Advances in Nondestructive Testing* 12: 95-116. New York, N.Y.: Gordon and Breach Science.

Gunasekaran, S., T. M. Cooper, A. G. Berlage, and P. Krishnan. 1987. Image processing for stress cracks in corn kernels. *Trans. ASAE* 30(1): 266-271.

Gunasekaran, S., T. M. Cooper, and A. G. Berlage. 1988. Soybean seed coat and cotyledon crack detection by image processing. *J. Agric. Eng. Res.* 41(2): 139-148.

Haff, R. P., and D. C. Slaughter. 2002. X-ray inspection of wheat for granny weevils: Real-time digital imaging vs. film. ASAE Paper No. 026093. St. Joseph, Mich.: ASAE.

Haff, R. P., and D. C. Slaughter. 2004. Real-time x-ray inspection of wheat for infestation by granary weevil, *Sitophilus granarius* (L.). *Trans. ASAE* 47(2): 531-537.

Karunakaran, C., D. S. Jayas, and N. D. G. White. 2003a. Soft x-ray inspection of wheat kernels infested by *Sitophilus oryzae*. *Trans. ASAE* 46(3): 739-745.

Karunakaran, C., D. S. Jayas, and N. D. G. White. 2003b. X-ray image analysis to detect infestations caused by insects in grain. *Cereal Chem.* 80(5): 553-557.

Karunakaran, C., D. S. Jayas, and N. D. G. White. 2004. Identification of wheat kernels damaged by red flour beetle using x-ray images. *Biosystems Eng.* 87(3): 267-274.

Kim, S., and T. Schatzki. 2001. Detection of pinholes in almonds through x-ray imaging. *Trans. ASAE* 44(4): 997-1003.

Tao, Y., Z. Chen, H. Jing, and J. Walker. 2001. Internal inspection of deboned poultry using x-ray imaging and adaptive thresholding. *Trans. ASAE* 44(4): 1005-1009.

Thomas, P., A. Kannan, V. H. Degwekar, and M. S. Ramamurthy. 1995. Non-destructive detection of seed weevil-infested mango fruits by x-ray imaging. *Postharvest Biol. Tech.* 5(1): 161-165.

Wan, Y. N., C. M. Lin, and J. F. Chiou. 2002. Rice quality classification using an automatic grain quality inspection system. *Trans. ASAE* 45(2): 379-387.